Predicting Chemical Shifts in Proteins: Structure Refinement of Valine Residues by Using *ab Initio* and Empirical Geometry Optimizations†

John G. Pearson,‡ Hongbiao Le,¶ Lori K. Sanders, Nathalie Godbout, Robert H. Havlin,# and Eric Oldfield*

Contribution from the Department of Chemistry, University of Illinois at Urbana−Champaign, 600 South Mathews Avenue, Urbana, Illinois 61801-3364

Received May 6, 1997. Revised Manuscript Received September 9, 1997⊗

Abstract: We have investigated the carbon-13 solution nuclear magnetic resonance (NMR) chemical shifts of C^{α}, C^{β}, and C^{γ} carbons of 19 valine residues in a vertebrate calmodulin, a nuclease from *Staphylococcus aureus*, and a ubiquitin. Using empirical chemical shift surfaces to predict C^{α}, C^{β} shifts from known, X-ray ϕ,ψ values, we find moderate accord between prediction and experiment. *Ab initio* calculations with coupled Hartree−Fock (HF) methods and X-ray structures yield poor agreement with experiment. There is an improvement in the *ab initio* results when the side chain χ_1 torsion angles are adjusted to their lowest energy conformers, using either *ab initio* quantum chemical or empirical methods, and a further small improvement when the effects of peptide-backbone charge fields are introduced. However, although the theoretical and experimental results are highly correlated ($R^2 \sim 0.90$), the observed slopes of $\sim -0.6-0.8$ are less than the ideal value of -1, even when large uniform basis sets are used. Use of density functional theory (DFT) methods improves the quality of the predictions for both C^{α} (slope $= -1.1$, $R^2 = 0.91$) and C^{β} (slope $= -0.93$, $R^2 = 0.89$), as well as giving moderately good results for C^{γ}. This effect is thought to arise from a small, conformationally-sensitive contribution to shielding arising from electron correlation. Additional shielding calculations on model compounds reveal similar effects. Results for valine residues in interleukin-1β are less highly correlated, possibly due to larger crystal−solution structural differences. When taken together, these results for 19 valine residues in 3 proteins indicate that choosing the lowest energy χ_1 conformer together with X-ray ϕ,ψ values enables the successful prediction of both C^{α} and C^{β} shifts, with DFT giving close to ideal slopes and R^2 values between theory and experiment. These results strongly suggest that the most highly populated valine side-chain conformers are those having the lowest (computationally determined) energy, as evidenced by the ability to predict essentially all C^{α}, C^{β} chemical shifts in calmodulin, SNase, and ubiquitin, as well as moderate accord for C^{γ}. These observations suggest a role for chemical shifts and energy minimization/geometry optimization in the refinement of protein structures in solution, and potentially in the solid state as well.

Introduction

Over the past few years there has been increasing interest in predicting chemical shifts in proteins, using both empirical and *ab initio* quantum chemical methods.[1−3] For ^{1}H NMR, chemical shifts are dominated primarily by local electrostatic field and magnetic anisotropy effects,[4,5] while for ^{13}C NMR, it is the local torsion angles which dominate shielding.[2,3,6,7] This connection between structure and shielding (or chemical shift) is clearly an important one since it means that chemical shifts should be calculable if a structure is known, permitting validation of spectral assignments, and that elements of structure should be predictable if shifts are known.

In earlier work, we showed that generally good agreement between experimental and *ab initio* theoretical shifts could be obtained for alanine residues in a *Staphylococcal* nuclease and calmodulin, and for valine residues in calmodulin.[2,6−8] However, in more recent work, we have found that in several cases the chemical shifts of valine residues in proteins are in poor accord with experiment, with the errors increasing from C^{α} to C^{β} to C^{γ}. It appeared to us that, in principle, there could be four main causes of these discrepancies. First, the input structures, typically obtained from the results of single-crystal X-ray diffraction measurements, might simply be inaccurate. Second, they might be accurate but might be a poor representation of the local solution structure. Third, there could be problems associated with motional averaging, either in the crystals or in solution. And fourth, there might be a deficiency in the theoretical methods used previously. The accuracy of protein X-ray structures can be assessed in several ways, one of the more useful being an analysis of the pooled standard deviations of helical ϕ,ψ and χ_1 angles, which correlate strongly with crystallographic resolution and refinement (R factors).[9] These results strongly indicate that only the very best structures can be expected to produce accurate chemical shift results—assuming of course that crystal and solution structures are in fact comparable. For the X-ray structures, χ_1 deviations

† This work was supported by the United States Public Health Service (Grant No. GM-50694).

‡ American Cancer Society Fellow. Present address: Department of Physiology, Johns Hopkins Medical Center, Baltimore, MD 21205-2183.

¶ Present address: Laboratorium für Physikalische Chemie, Universitatstrasse 22, 8092, Zürich, Switzerland.

Barry Goldwater Fellow.

⊗ Abstract published in *Advance ACS Abstracts,* November 15, 1997.

(1) Wishart, D. S.; Sykes, B. D.; Richards, F. M. *Biochemistry* **1992**, *31*, 1647−1651.

(2) de Dios, A. C.; Pearson, J. G.; Oldfield, E. *Science* **1993**, *260*, 1491−1496.

(3) Oldfield, E. *J. Biomol. NMR* **1995**, *5*, 217−225.

(4) Ösapay, K.; Case, D. A. In *Nuclear Magnetic Shielding and Molecular Structure*; Tossell, J. A., Ed.; Kluwer Academic Publishers; Dordrecht, The Netherlands, 1993; p 572.

(5) Williamson, M. P.; Asakura, T.; Nakamura, E.; Demura, M. *J. Biomol NMR* **1992**, *2*, 83−98.

(6) de Dios, A. C.; Pearson, J. G.; Oldfield, E. *J. Am. Chem. Soc.* **1993**, *115*, 9768−9773.

(7) de Dios, A. C.; Oldfield, E. *J. Am. Chem. Soc*. **1994**, *116*, 5307−5314.

(8) Laws, D. D.; de Dios, A. C.; Oldfield, E. *J. Biomol. NMR* **1993**, *3*, 607−612.

S0002-7863(97)01461-3 CCC: $14.00

are considerably larger than ϕ,ψ deviations.[9] For NMR structures, ϕ,ψ values are somewhat more scattered than in X-ray structures,[10] and pooled χ_1 standard deviations are similarly larger.[11] In many cases, this may be attributable to enhanced conformer averaging in solution.

From the standpoint of refining or predicting aspects of protein structure, it is clearly of interest to know how best to predict a spectrum, since there are in principle both static structural questions and dynamical averaging questions, as well as in some cases questions as to what level of theory needs to be used to evaluate a particular property. Here, we focus on the basic question of how to calculate C^α, C^β, and C^γ carbon-13 chemical shifts of valine residues in proteins having moderately good resolution (~1.5 Å) crystal structures. In previous work, we found relatively good accord for valine C^α sites in calmodulin, but specific assignments to a given χ_1 were difficult, relying on absolute shielding arguments and comparisons with shifts for alanine. Moreover, agreement for C^β was rather poor, as was the case for C^γ.

In this paper, we resolve some of the problems encountered previously. Specifically, we test the following hypothesis: that the backbone structures of proteins in solution are generally well defined by X-ray ϕ,ψ values from high-resolution structures, but that χ_1 torsions (in valine) are poorly described. The basis for constructing this hypothesis is as noted above—X-ray structures have quite "tight" ϕ, ψ, χ_1 distributions, and these distributions get tighter as the crystallographic resolution and *R* factors improve. We believe this implies that it should be possible, and in fact essential, to try to extrapolate these structural parameters to their error free values, that is to say their equilibrium values, a process which one can, in principle, begin to address by using geometry optimization. Since the χ_1 pooled deviations are larger than the ϕ,ψ deviations, and the NMR structure families encompass even larger regions of conformational space, we simply fix ϕ,ψ to the protein X-ray values and optimize χ_1. If there is extensive dynamical averaging or crystal−solution structural differences, this approach will fail. However, we do in fact find that good correlations (R^2 values) between experimental solution and X-ray predicted chemical shifts (or shieldings) can be made by selecting the lowest energy χ_1 structures, obtained from *ab initio* geometry optimization or force fields. The overall best theory-versus-experimental results are obtained by using density functional theory (DFT), where close to ideal slopes **and** R^2 values are achieved with **both** coupled sum-over-states density functional perturbation theory (SOS-DFT, as implemented in deMon[12]) and uncoupled (in Gaussian 94[13]) approaches. In recent work by Liu et al.,[14] it has also been clearly shown that—even in very high resolution single crystal X-ray and neutron diffraction structures of small molecules (methyl glycosides), that *ab initio* geometry optimization permits a major improvement in chemical shielding *tensor* element predictions with quantum chemical methods, and Facelli and Grant have reported a similar conclusion for naphthalene.[15] For proteins, however, the situation is even more complex, since not only are the initial structures less well resolved than with small molecules, but it is also necessary to consider the effects of crystal−solution structural nonequivalencies.

Experimental Section

Empirical Surfaces. For our empirical predictions of C^α, C^β shifts we used a global data base of C^α, C^β shieldings, which contains the shifts of 975 amino acids.

Ab Initio Calculations. We used three different approaches to evaluate ^{13}C shieldings of valine residues in proteins: Coupled Hartree−Fock (CHF) in the Texas suite of programs of Pulay et al.;[16,17] SOS-DFPT, using the individual gauge for localized orbitals (IGLO) approach;[12] and uncoupled DFT in Gaussian 94,[13] using gauge including atomic orbitals (GIAOs). In each case, we investigated the *N*-formylvaline amide molecule shown below:

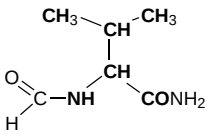

In the CHF calculations we used a locally dense basis approach,[18] basically as described previously: 6-311G** on the atoms shown in bold above, with a 6-31G** basis on the other atoms. In the deMon SOS-DFPT-IGLO shielding calculations we used an IGLO-III basis[19] on all atoms, together with the PW91 exchange-correlation functional[20] and a fine grid.[12] In the Gaussian 94 DFT-GIAO shielding calculations, we used a uniform (6-311++G(2d,2p)) basis on all atoms, together with the BPW91 energy functional.[13] Selected locally dense basis set calculations were also performed, as discussed below.

The actual valine geometries used varied considerably, and are discussed in more detail in the text. For our initial shielding calculations with CHF we used torsion angles for calmodulin, SNase, and ubiquitin taken directly from the Brookhaven Protein Data Bank (ref 21 ; Files 1cll, lsnc, and lubq), while standard bond lengths and three-atom angles were from an AMBER[22] force field in the Discover program (Biosym Technologies, San Diego, CA). As we have shown previously, bond lengths adjusted to fixed values permit more precise shielding predictions than do some X-ray structure bond angles, so for our initial calculations the same procedure as used previously was adopted.

We used three different approaches to investigate the effects of geometry optimization/structure refinement on ^{13}C shielding. First, we adjusted the χ_1 torsions to their closest staggered conformer values: −60°, 60°, or 180°. Second, we used an AMBER force field in Discover, combined with a conjugate gradient minimization, to produce an empirical χ_1 optimization, centered around each of the three likely χ_1 values. Third, we carried out a full *ab initio* geometry optimization at the X-ray fixed ϕ,ψ angles, using Hartree−Fock theory (Gaussian

(9) Morris, A. L.; MacArthur, M. W.; Hutchinson, E. G.; Thornton, J. M. *Proteins* **1992**, *12*, 345−364.

(10) Thornton, J. M.; Hutchinson, E. G.; Jones, S.; Laskowski, R. A.; MacArthur, M.; Michie, A.; Orengo, C. M.; Rullman, J. A. C.; Kaptein, R. *XVIIth International Conference on Magnetic Resonance in Biological Systems*; Keystone, CO, 1996; Abstracts, p 66.

(11) MacArthur, M. W.; Thornton, J. M. *Proteins* **1993**, *17*, 232−251.

(12) Malkin, V. G.; Malkina, O. L.; Casida, M. E.; Salahub, D. R. *J. Am. Chem. Soc.* **1994**, *116*, 5898−5908.

(13) Frisch, M. J.; Trucks, G. W.; Schlegel, H. B.; Gill, P. M. W.; Johnson, B. G.; Robb, M. A.; Cheeseman, J. R.; Keith, T.; Petersson, G. A.; Montgomery, J. A.; Raghavachari, K.; Al-Laham, M. A.; Zakrzewski, V. G.; Ortiz, J. V.; Foresman, J. B.; Cioslowski, J.; Stefanov, B. B.; Nanayakkara, A.; Challacombe, M.; Peng, C. Y.; Ayala, P. Y.; Chen, W.; Wong, M. W.; Andres, J. L.; Replogle, E. S.; Gomperts, R.; Martin, R. L.; Fox, D. J.; Binkley, J. S.; Defrees, D. J.; Baker, J.; Stewart, J. P.; Head-Gordon, M.; Gonzalez, C.; Pople, J. A. *Gaussian94/DFT*; Gaussian, Inc.: Pittsburgh, PA, 1995.

(14) Liu, F.; Phung, C. G.; Alderman, D. W.; Grant, D. M. *J. Am. Chem. Soc.* **1996**, *118*, 10629−10634.

(15) Facelli, J. C.; Grant, M. *Nature* **1993**, *365*, 325−327.

(16) Wolinski, K.; Hinton, J. F.; Pulay, P. *J. Am. Chem. Soc.* **1990**, *112*, 8251−8260.

(17) Pulay, P.; Wolinski, K.; Hinton, J. F. *The Texas Program*; University of Arkansas, Fayetteville, AR, 1991, 1993.

(18) Chestnut, D. B.; Moore, K. D. *J. Comput. Chem.* **1989**, *10*, 648−659.

(19) Kutzelnigg, W.; van Wüllen, Ch.; Fleishcher, U.; Franke, R.; Mourik, T. v. In *Nuclear Magnetic Shieldings and Molecular Structure*; Tossell, J. A., Ed.; Kluwer Academic Publisher: Dordrecht, The Netherlands, 1993; pp 141−161. van Wüllen, Ch.; Kutzelnigg, W. *User's Manual for IGLO*, This program and documentation is part of MOLPRO by J.-J. Werner and P. J. Knowles, University of Sussex, 1992.

(20) Perdew, J. P.; Wang, Y. *Phys. Rev. B* **1986**, *33*, 8800−8802. Perdew, J. P. *Phys. Rev. B* **1986**, *33*, 8822−8824.

(21) Abola, E. E.; Bernstein, F. C.; Bryant, S. H.; Koetzle, T. F.; Weng, J. Protein Data Bank. In *Crystallographic Databases—Information Content, Software Systems, Scientific Applications*; Data Commission of the International Union of Crystallography.

(22) Weiner, P. K.; Kollman, P. A. *J. Comput. Chem.* **1981**, *2*, 287−303. Brooks, B. R.; Bruccoleri, R. E.; Olafson, B. D.; States, D. J.; Swaminathan, S.; Karplus, M. *J. Comput. Chem.* **1983**, *4*, 187−217.

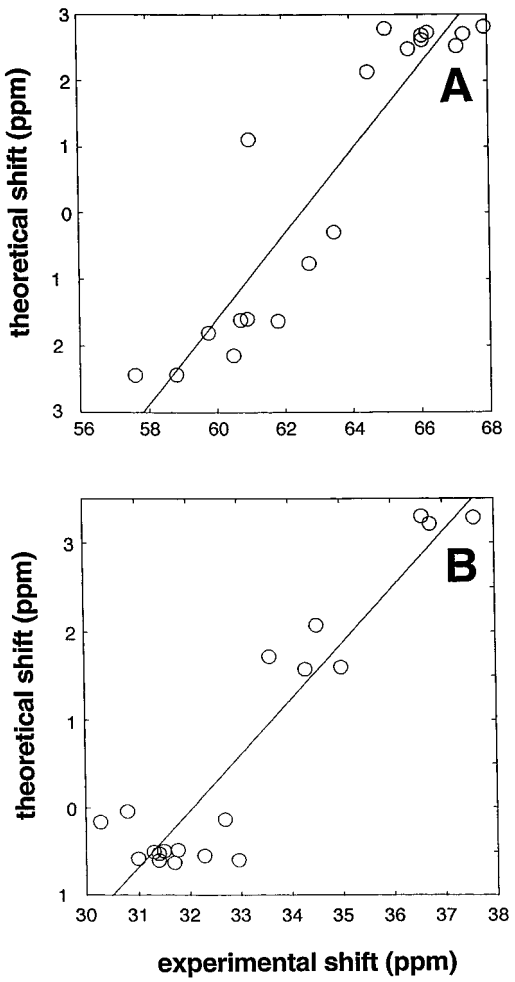

Figure 1. Graph showing correlation between experimental valine chemical shifts (in ppm from tetramethylsilane, TMS, corrected as discussed in the text) in calmodulin, SNase, and ubiquitin and secondary chemical shifts, obtained from a global data base of 975 amino acid residues: (A) C^{α} (slope = 0.64, R^2 = 0.85); (B) C^{β} (slope = 0.63, R^2 = 0.87).

94) with a uniform 6-31G basis. Computations were carried out with IBM RS/6000 (International Business Machines Corporation, Austin, TX) RISC workstations, Models 340, 350, 365, and 3CT, with external National Peripherals (MTI, Chicago, IL) disc drives, and on a Silicon Graphics (Mountain View, CA) Origin-2000 4-processor system, in this case with parallel processing. Texas software was kindly provided by Professors P. Pulay, J. F. Hinton, and Dr. K. Wolinski; and the deMon code was from Professor D. Salahub and Drs. V. G. Malkin, O. L. Malkina, and E. Proynov.

Results and Discussion

We first investigated the use of empirical chemical shift surfaces to predict valine C^{α} and C^{β} shifts in proteins, using the X-ray determined ϕ,ψ torsion angle values. As can be seen from Figure 1 and Table 1 (**1**), the slope and R^2 values are moderately good, with the main deficiency being in the slopes, of 0.63 to 0.64, versus the ideal value of 1. However, it is difficult to see how to make major improvements, since as shown by Williamson et al., individual valine χ_1 shift surfaces are essentially indistinguishable,[23] even though *ab initio* computed shielding surfaces for the three valine χ-conformers are clearly very different.[24] Moreover, there is no information available on the shielding tensor elements, which as we note briefly below are highly ϕ, ψ, χ_1 sensitive. The reason for the similarity of the three empirical χ_1 valine C^{α} shielding surfaces is almost certainly "χ_1 noise". That is, a significant fraction of the valine side chains in the crystallographic data base have *different* χ_1 values in solution (where the shifts are actually determined) and in the crystalline solid state (where the ϕ,ψ values are determined). An immediate prediction of this hypothesis is that *ab initio* calculations of C^{α}, C^{β}, and C^{γ} shifts will likewise also be noisy—having poor R^2 values, as well as small slopes, associated with these low "goodness of fit" coefficients. This is exactly the result found, as shown in Table 1 (**2**), where we show the slope and R^2 values for the same 19 valine residues, this time predicted from the C^{α} and C^{β} shielding hypersurfaces reported previously.[24] The results for C^{α} are poor and those for C^{β} are even worse. To investigate whether this could also be due to a basis set deficiency, we then carried out individual shielding calculations using coupled Hartree−Fock (CHF) theory in the Texas program, using the large, locally dense basis described above. Again, the results were unimpressive Figure 2, Table 1 (**3**)).

We then reasoned that perhaps many of the unusual χ_1 torsions detected in the X-ray structures were in fact of too high an energy and were unphysical, being associated with the use of relatively low resolution crystal structures. However, χ_1 torsion errors of say 15° only have a minor effect on shielding, since we know the shapes of the shielding derivatives close to their staggered minima,[6] and these derivatives are small around $\chi_1 = \pm 60°, 180°$.[6] To obtain much better slope and R^2 values (ideally −1.0, 1.0), it appeared that much larger χ_1 rotations must be necessary, or that some other factor was being omitted in the calculation—or maybe both. To test the former idea, we set the χ_1 torsions to the staggered conformations ($\chi_1 = \pm 60°$, 180°) closest to the values found in the X-ray structures for SNase and ubiquitin, and closest to the values found with *J*-couplings for calmodulin. Calmodulin V55 was treated as a 1:1 mixture of fragments having $\chi_1 = 180°$ and $\chi_1 = -60°$ as a crude way to include conformer averaging, since V55 is in a mobile loop. Shieldings were then recomputed, producing a major overall improvement in R^2 values (0.86, 0.79) , Table 1 (**4**), but the −0.44 slope for C^{β} remained troubling.

The next step was to try to directly use computational methods to refine the structures of the valine fragments, using energy as a discriminator. Of course, in systems as complex as proteins, where dynamical and solvent interactions might both be important in controlling the type of conformational ensemble present, this approach is perhaps oversimplified. However, we are testing a hypothesis, and since in unpublished work[25] we have found no instances in which molecular dynamics methods provide any improvement in C^{α} shielding, it seemed worth exploring the possibility that finding the lowest energy local structure might improve the agreement between experimental and theoretical chemical shifts.

We therefore calculated the total eigenenergies for the X-ray as well as the three "standard" χ_1 conformations of each of the 19 valine sites, with the results obtained being shown in Table S1 (Supporting Information). As can be seen in Table S1, in essentially all cases lowest or equal lowest energies are obtained for one of the standard geometries, as opposed to the reported X-ray geometries. Also, these standard geometries give improved correlations between theory and experiment, Table 1 (**4**). These observations strongly suggest that by using energy as a discriminator, structures which more accurately reflect solution structures can be deduced.

The largest differences between the X-ray and lowest energy χ_1 conformations occur in calmodulin, with in particular the 180° conformer being selected in all seven cases, similar to the

(23) Williamson, M.; Asakura, T. *XVIIth International Conference on Magnetic Resonance in Biological Systems*, Keystone, CO, 1996; Abstracts, page 62.

(24) Laws, D. D.; Le, H.; de Dios, A. C.; Havlin R. H.; Oldfield, E. *J. Am. Chem. Soc.* **1995**, *117*, 9542−9546.

(25) McMahon, M.; Oldfield, E. Unpublished results.

Table 1. Slope and R^2 Values of Experimental ^{13}C Chemical Shifts versus Theoretical Shieldings for C^α and C^β Carbons in Valine[a]

			slope	R^2	intercept (ppm)
1	expt. vs. global empirical (X-ray)	C^α	0.64[b]	0.85	
	expt vs global empirical (X-ray)	C^β	0.63[b]	0.87	
2	expt vs hypersurface (X-ray)	C^α	−0.56	0.45	176.6
	expt vs hypersurface (X-ray)	C^β	−0.32	0.08	181.1
3	expt vs Texas (X-ray)	C^α	−0.66	0.45	181.2
	expt vs Texas (X-ray)	C^β	−0.45	0.15	179.5
4	expt vs Texas (lowest energy, standard χ_1)	C^α	−0.82	0.86	188.5
	expt vs Texas (lowest energy, standard χ_1)	C^β	−0.44	0.79	177.5
5	expt vs Texas (Discover, lowest energy χ_1)	C^α	−0.70	0.87	180.6
	expt vs Texas (Discover, lowest energy χ_1)	C^β	−0.59	0.78	182.3
6	expt vs Texas (G94, 631-G optimized)	C^α	−0.86	0.90	194.1
	expt vs Texas (G94, 631-G optimized)	C^β	−0.58	0.78	183.2
7	expt vs Texas (G94, optimized; charge field)	C^α	−0.89	0.92	196.3
	expt vs Texas (G94, optimized; charge field)	C^β	−0.64	0.90	185.3
8	expt vs G94 DFT (G94, optimized)	C^α	−1.05	0.88	186.9
	expt vs G94 DFT (G94, optimized)	C^β	−0.80	0.74	170.7
9	expt vs deMon DFT (G94, optimized)	C^α	−1.10	0.89	188.5
	expt vs deMon DFT (G94, optimized)	C^β	−0.84	0.76	170.9
10	expt vs. deMon DFT (G94, optimized; charge field)	C^α	−1.09	0.91	188.1
	expt vs deMon DFT (G94, optimized; charge field)	C^β	−0.93	0.89	173.9

[a] Nineteen valine residue in a vertebrate calmodulin, a nuclease from *Staphylococuus aureus*, and a ubiquitin. The experimental chemical shifts are from refs 32, 33, and 34. The following shift corrections were applied to the experimental shifts: calmodulin, −0.1 ppm; Snase, 0.0 ppm; and ubiquitin, −0.5 ppm. A −0.1 ppm correction means that 0.1 ppm was added to the reported experimental shift.

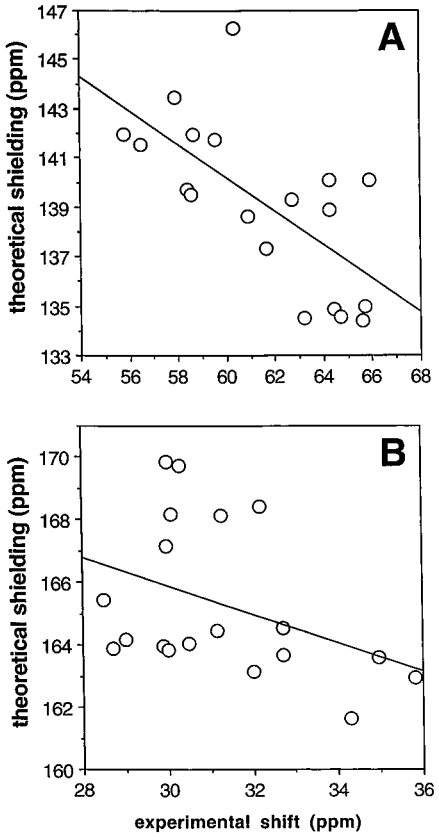

Figure 2. Graph showing correlation between experimental valine chemical shifts and theoretical shieldings computed with CHF theory (Texas program) with raw PDB X-ray structures: (A) C^α (slope = −0.66, R^2 = 0.45) and (B) C^β (slope = −0.45, R^2 = 0.15).

J-coupling results,[26] and our previous analysis of C^α shieldings.[7] For Val 55, the energies for $\chi_1 = 180°, -60°$ are within 0.1 kcal of each other, consistent with our use of a 1:1 conformational average for its computed shieldings (see above). We then further investigated the use of geometry optimization, using both an empirical and a quantum chemical method. We first optimized fragment structures using the Amber force field, fixing the peptide backbone at the X-ray ϕ,ψ values. In this way, we obtained structures which are only optimized for the χ_1 rotation. Each of the three standard χ_1 conformations were used as starting points for the minimization. The resulting structures were then used as input for CHF calculations of energy and shielding. The energy results are shown in Table 2, and the chemical shielding results are shown in Figure 3 and Table 1 (**5**). We then carried out a further stage of geometry optimization, by taking the lowest energy conformers from the Amber/Discover optimization and carrying out a full geometry optimization using the CHF method in Gaussian 94. The energies obtained are given in Table 2, and a comparison between experimental shifts and theoretical shieldings is given in Figure 4 and Table 1 (**6**).

As can be seen in Figure 3 and Table 1 (**5**), use of the Discover optimized structures results in a small improvement in slope and R^2 over the fixed χ_1 results, but the slopes of −0.7 for C^α and −0.59 for C^β are far less than the ideal value of −1.0. However, a full geometry optimization results in slopes of −0.86 (C^α) and −0.58 (C^β), as well as good R^2 values (0.9, 0.78), an improvement in C^α slope with respect to the force field optimizations, due presumably to the larger shielding derivatives for C^α. The energies are also uniformly lower, Table 2, due to relaxation of the bond length constraints. We summarize in Table 3 the χ_1 results obtained. There are only four major (>120°) χ_1 changes, all in calmodulin. Moreover, use of either empirical or full *ab initio* geometry optimization permits not only selection of the most probable conformer but also improved predictions for both C^α and C^β chemical shifts. However, bond length effects are small (unless strong hydrogen bonding is involved, ref 27) so there remains a problem with the slope of C^β.

We next investigated at the CHF level the effects of incorporating a local charge field. We incorporated partial atomic charges (AMBER force field) on peptide groups, since these are expected to have the largest effects on shielding. When this charge-field perturbation is used there are small improvements in slope and R^2, Figure 5 and Table 1 (**7**), although for C^β the slope of −0.64 is still considerably less than the ideal value of −1.0, suggesting the possibility of a missing ingredient in the calculations. One possibility is that the basis is still not saturated. We therefore carried out shielding calculations for C^α and C^β on nine randomly selected residues using a dense 6-311++G(2d,2p) basis on all atoms. The effects were very small—a 6% decrease in shielding range for C^α, and no effect for C^β. The missing ingredient seemed, therefore, not be a basis

(26) Ikura, M. Private communication. Ikura, M.; Spera, S.; Barbato, G.; Kay, L. E.; Krinks, M.; Bax, A. *Biochemistry* **1991**, *30*, 9216−9228. Vuister, G. W.; Wang, A. C.; Bax, A. *J. Am. Chem. Soc.* **1993**, *115*, 5334−5335.

(27) de Dios, A. C.; Oldfield, E. *J. Am. Chem. Soc.* **1994**, *116*, 11485−11488.

Table 2. Calculated energies of N-Formylvaline Amide Fragments in Calmodulin, Staphylococcal Nuclease, and Calmodulin, Calculated at the SCF Level (Texas Program, Locally Dense Basis Sets) for different Geometry Optimized Structures

			energy (kcal/mol)[b]					
			empirical			*ab initio*		
residue[a]		X-ray	180 (min)	−60 (min)	60 (min)	180 (gopt)	−60 (gopt)	60 (gopt)
calmodulin	35	−315.4	−315.6	−313.7	−314.1	−319.3		
	55	−312.7	−314.9	−315.9	−315.1	−319.2	−321.1	
	91	−312.2	−316.5	−315.7	−315.8	−320.0		
	108	−310.2	−316.6	−316.1	−316.3	−319.7		
	121	−316.0	−316.3	−315.2	−315.4	−320.3		
	136	−310.5	−320.4	−319.3	−319.3	−323.9		
	142	−309.2	−316.4	−315.5	−315.7	−319.9		
SNase	23	−317.9	−319.1	−320.6	−320.6		−324.2	
	39	−318.8	−315.7	−320.4	−318.6		−324.1	
	66	−314.9	−316.5	−316.5	−316.2		−320.9	
	74	−318.6	−319.9	−320.0	−319.5		−323.6	
	99	−316.1	−316.3	−315.2	−315.5	−319.8		
	104	−315.5	−315.6	−313.8	−314.2	−319.3		
	111	−318.4	−319.4	−318.0	−318.2	−323.2		
	114	−319.9	−320.2	−318.4	−318.6	−323.9		
ubiquitin	5	−320.3	−320.3	−318.9	−323.9			
	17	−319.6	−316.0	−320.5	−318.9		−324.2	
	26	−315.4	−315.7	−314.2	−314.6	−319.4		
	70	−319.5	−319.8	−319.7	−319.3	−323.3		

[a] The structures used were the following: calmodulin, PDB File 1cll; SNase, PDB File 1snc; ubiquitin, PDB File 1ubq. [b] The energies given are the total SCF molecular eigenenergies, plus 309 000 kcal/mol. The empirical geometry optimizations were performed with the AMBER forcefield (Insight program in Discover). The *ab initio* geometry optimizations were as described in the text; HF 6-311G uniform basis. Large locally dense basis sets were used for the energy (and shift) calculations; see the Experimental Section for more details.

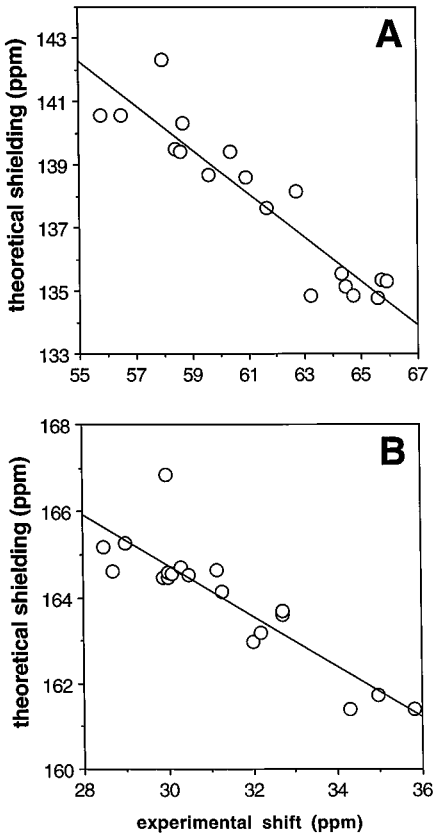

Figure 3. Graph showing correlation between experimental valine chemical shifts and theoretical shieldings computed with CHF theory (Texas program) using valine fragments having χ_1 angles set using the Discover program: (A) C^α (slope = −0.70, R^2 = 0.87) and (B) C^β (slope = −0.59, R^2 = 0.78).

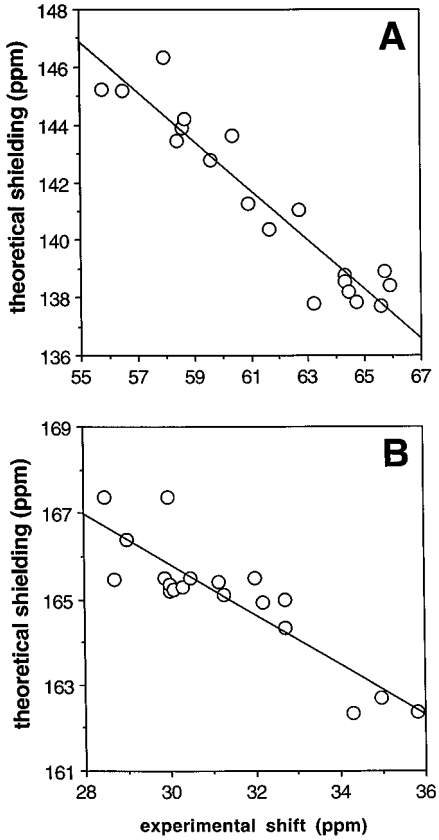

Figure 4. Graph showing correlation between experimental valine chemical shifts and theoretical shieldings computed with CHF theory (Texas program) with Gaussian 94 HF geometry optimized structures: (A) C^α (slope = −0.89, R^2 = 0.90) and (B) C^β (slope = −0.58, R^2 = 0.77).

or geometry effect, but perhaps originated in the neglect of another contribution to shielding.

Density Functional Theory Calculations

The major effects of electron correlation or shielding for light elements are seen primarily in multiple bonded situations such as CO, O_3, etc. However, the effects we are looking for are very small, on the order of 1−2 ppm, and are conformationally sensitive. The **major** shielding changes, due e.g. to C^α, C^β nonequivalence, are well described at the CHF level, where we find for example a good global slope when Ala, Val, C^α/C^β results are all considered together.[7] However, the CHF results do not always appear to provide the correct slope for a given site, with the largest errors being found for C^β of valine.

We therefore decided to investigate whether there might be conformationally sensitive contributions to the shielding calcula-

Table 3. Comparison between Valine χ_1-Angles in X-ray Structures and Those Obtained by Selecting the Lowest Energy Conformers Using Empirical and *ab Initio* Geometry Optimization Techniques

protein[a]	residue	χ_1(X-ray) (deg)	χ_1(geom opt) (deg)	$\lvert\Delta\chi_1\rvert$[b] (deg)
calmodulin	V35	173.9	172.1	1.8
	V91	47.9	171.9	124.0
	V108	−39.2	171.9	148.9
	V136	−28.6	176.4	155.0
	V142	−39.6	171.7	148.7
SNase	V23	−47.4	−69.6	22.2
	V39	−51.0	−63.6	12.6
	V66	−60.2	−65.5	5.3
	V74	−59.0	−69.4	10.4
	V99	177.6	171.7	5.9
	V104	174.4	172.0	2.4
	V111	164.3	175.5	11.2
	V114	−177.4	178.0	4.6
ubiquitin	V5	−179.8	178.0	2.2
	V17	−62.5	−63.7	1.2
	V26	168.2	171.9	3.7
	V70	177.0	175.1	1.9

[a] The structures used were as follows: calmodulin, PDB File 1cll; SNase, PDB File 1snc; and ubiquitin, PDB File 1 ubq. [b] Difference between X-ray χ_1 and geometry optimized value.

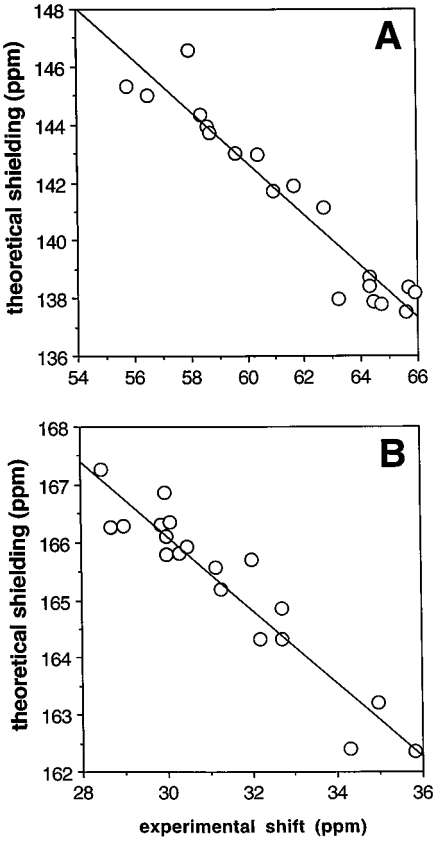

Figure 5. Graph showing correlation between experimental valine chemical shifts and theoretical shieldings computed with CHF theory (Texas program) using Gaussian 94 geometry optimized valine fragments in the presence of a peptide charge field: (A) C^{α} (slope = −0.89, R^2 = 0.92); (B) C^{β} (slope = 0.64, R^2 = 0.90).

tions which were method dependent by evaluating C^{α} and C^{β} chemical shifts in three model systems: propanal (**1**), propionamide (**2**), and *N*-ethylformamide (**3**):

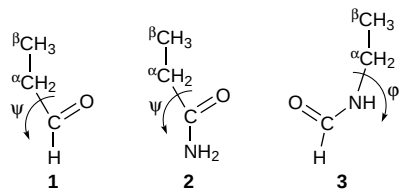

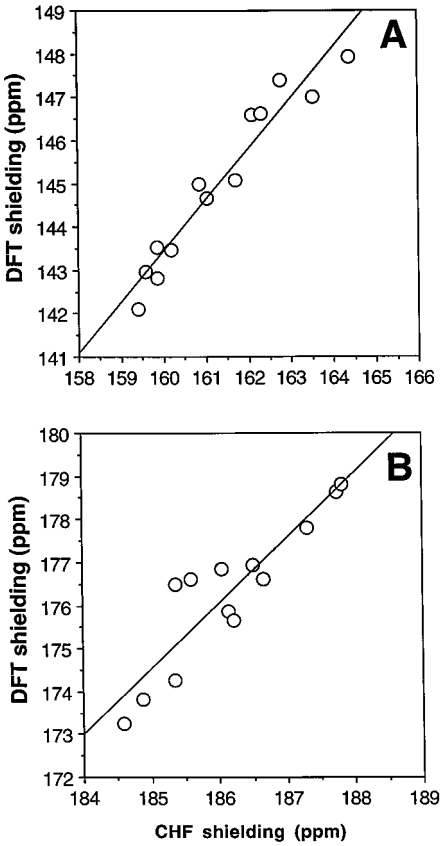

Figure 6. Graph showing correlation between ^{13}C shielding in propanal as a function of the O−C1−C2−C3 (ψ) torsion angle. Shielding values were computed via density functional theory (Gaussian 94, 6−311G optimization basis, uniform 6-311++G(2d, 2p) uniform shielding basis) and via HF theory (Texas program, 6-311++G(2d, 2p) uniform shielding basis): (A) C^{α}/C2 (slope = 1.22, R^2 = 0.95); and (B) C^{β}/C3 (slope = 1.85, R^2 = 0.86).

We thought that since there are large correlation effects within the carbonyl group there might also be small, residual effects due to correlation for neighboring atoms, especially those which come into close steric contact due to *conformational* changes, such as changes in the ψ torsion angle shown above. We selected 12 ϕ,ψ torsion angles for the above molecules and carried out a full HF geometry optimization (6-311G basis), then using a uniform 6-311++G(2d,2p) basis and gauge including atomic orbitals, we evaluated the C^{α} and C^{β} shieldings using CHF (Texas) and DFT (Gaussian 94). Typical results for C^{α} and C^{β} of propanal are shown in Figure 6. As can be seen, there is a wider range of chemical shielding for both C^{α} (A) and C^{β} (B) when DFT is used, with slopes of 1.22 (C^{α}) and 1.85 (C^{β}) for the DFT vs CHF comparison. For propionamide, we find slopes of 1.43 (C^{α}) and 1.75 (C^{β}), and for *N*-ethylformamide, 1.20 (C^{α}) and 0.91 (C^{β}). Although these are purely theoretical comparisons, they do suggest the possibility that at least part of the problem with the small slopes for C^{β} sites could reside in the method being used. We therefore next investigated C^{α} and C^{β} valine shieldings, using both coupled/SOS-DFPT/IGLO and uncoupled DFT/GIAO methods.

We show in Figure 7 and Table 1 (**8**) the results of C^{α} and C^{β} G94 (GIAO) DFT shielding calculations for 19 valine residues in calmodulin, SNase, and ubiquitin, using a CHF 6-31G geometry optimized fragment, evaluated in Gaussian 94 with a uniform 6-311++G(2d,2p) basis and the BPW91 functional.[13] Both the slope and R^2 values are very good, with noticeable improvements in the slope (-1.05, −0.80) being obtained in both cases. The scatter patterns in the CHF and DFT calculations track each other rather precisely, as shown in Figure 8, in which the DFT-GIAO results are plotted versus

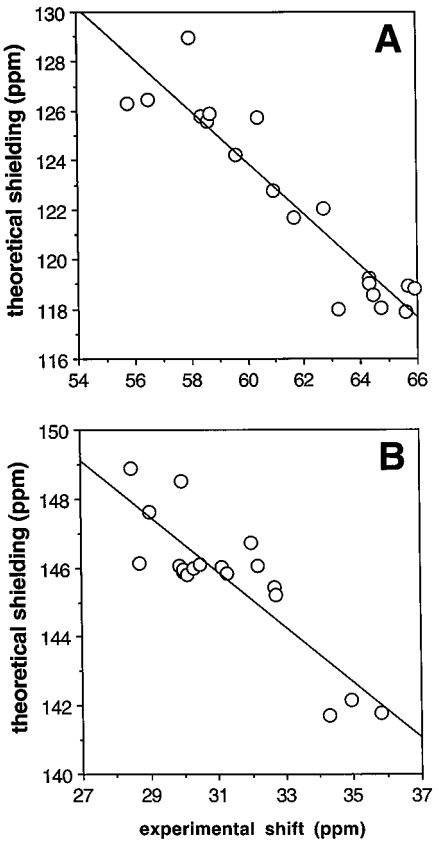

Figure 7. Graph showing correlation between experimental valine chemical shifts and theoretical shieldings computed with DFT theory (Gaussian 94 program) with a Gaussian 94 geometry optimized (HF 6-311G) input. (A) C^{α} (slope = −1.10, R^2 = 0.89); (B) C^{β} (slope = −0.83, R^2 = 0.76).

the CHF results, and where R^2 values of 0.994 (C^{α}) and 0.979 (C^{β}) are found. The main difference between the two calculations is in the slopes, which have values of 1.28 and 1.44, respectively. Essentially identical results for valine are also obtained with the SOS-DFPT approach, Table 1 (**9**), where we also investigated the effects of the peptide backbone local charge field, Figure 9 and Table 1 (**10**). Here, there is not only an improvement in slope, but a small improvement in R^2 values as well, Table 1 (**10**) (C^{α}, R^2 = 0.91; C^{β}, R^2 = 0.89). So, by using energy-selected, geometry optimized structures and by use of either coupled/SOS-DFPT (IGLO) or uncoupled/DFT (GIAO) approaches, it is possible to predict both C^{α} and C^{β} slopes with an error of ∼10%, and with R^2 values of ∼0.9. The absolute shieldings derived from these plots are also quite good, given that the intercepts (188, 174 ppm versus an ideal value of ∼186 ppm, ref 28) are due in large part to the slope of the conformational contribution to shielding. We present all of these slope and R^2 results for both C^{α} and C^{β}, as a function of increasing "quality" of the calculations—starting from raw X-ray data and a global, empirical data base, through density functional calculations in the presence of a local charge field on HF (6-311G) geometry optimized-energy selected molecules—in a graphical manner in Figure 10, where the *x*-axis correlates with the ten (**1**−**10**) types of calculations shown in Table 1. Best accord is obtained when χ_1 values are edited for the correct (major) conformer, the conformational spread is decreased by geometry optimization, bond lengths and bond angles are optimized, point charges are included, and a DFT method is used. However, HF methods are almost as good (column **7**, Texas program) if scaling corrections are allowed, since the R^2 values are also very high.

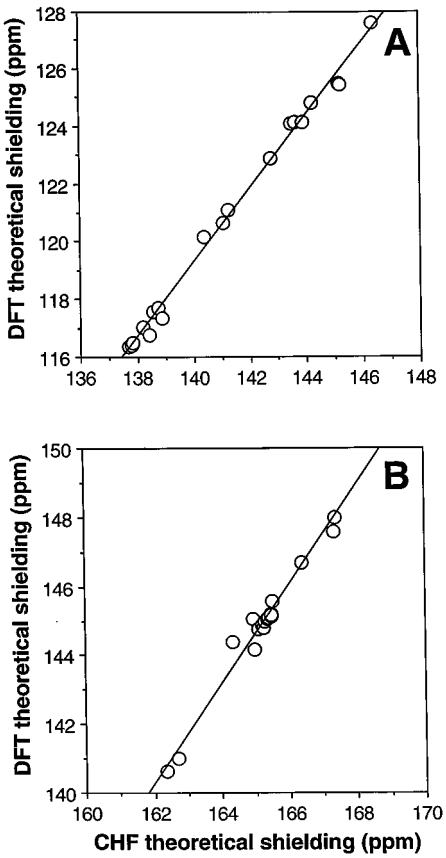

Figure 8. Comparison between HF GIAO (Texas) and SOS-DFPT-IGLO (deMon) computed shieldings for valine residues in proteins: (A) C^{α} (slope = 1.28, R^2 = 0.99); (B) C^{β} (slope = 1.44, R^2 = 0.98).

We also investigated the C^{α}, C^{β} shifts at the CHF level in the small cytokine interleukin-1β. For this protein, the predicted shieldings are in somewhat less good accord with experiment, and incorporation of the interleukin-1β calculations with those for the other three proteins reduces both the slope and R^2 values by about 5−10%. We do not think the effect is attributable to just χ_1 variation, since the interleukin-1β valine C^{α} shielding calculations are affected at least as much as those for C^{β}, suggesting involvement of ϕ and ψ as well. This effect is presumably due to either a lower resolution structure, crystal−solution structural differences, or dynamical effects, and at present we cannot differentiate between these possible effects. Further DFT calculations were not performed on IL-1β, since as we have shown above, the R^2 values between CHF and DFT approach unity, so DFT results would not improve R^2. The problem lies elsewhere. Crystal shifts of IL-1β would be one way to probe the question of crystal−solution nonequivalence, since if the structures are different, then the crystal and solution shifts will also be different.

The Shielding Tensors. We next discuss the individual shielding tensor elements, σ_{11}, σ_{22}, and σ_{33}, for a selection of 12 of the 19 valines (most helical calmodulins have been excluded, since their shieldings are so similar). The basic question of interest is the following: Do the differences between the CHF and DFT calculations arise from a major change in one tensor element, or are the effects rather uniform? In addition, it is of interest to briefly investigate how ϕ,ψ and χ_1 influence the shielding tensor elements since in favorable cases these may be determined experimentally, a topic we discuss elsewhere in some detail.[29,30] While $^{13}C^{\alpha}$, $^{13}C^{\beta}$ tensor information for proteins has not yet been reported, it should be

(28) Jameson, A. K.; Jameson, C. J. *Chem. Phys. Lett.* **1987**, *134*, 461−466.

(29) Havlin, R. H.; Le, C.; Laws, D. D.; deDios, A. C.; Oldfield, E. *J. Am. Chem. Soc.* **1997**, *119*, 11951−11958.

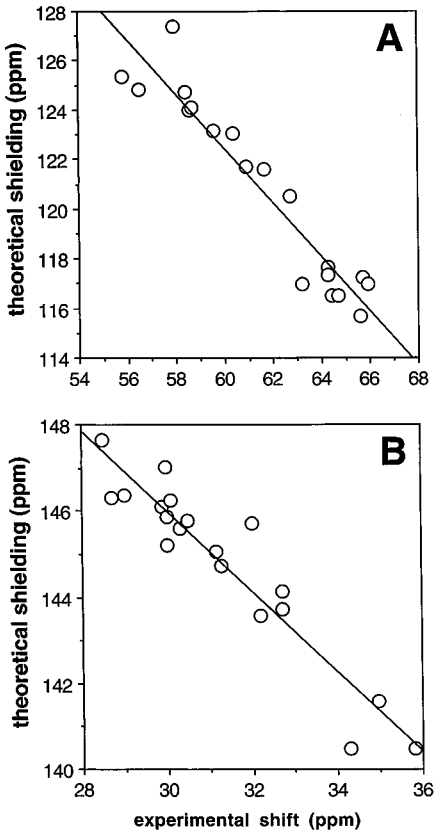

Figure 9. Graph showing correlation between experimental valine chemical shifts and theoretical shieldings computed with DFT theory (deMon program) using Gaussian 94 geometry optimized valine fragments and a local peptide charge field: (A) C^{α} (slope = −1.09, R^2 = 0.91); (B) C^{β} (slope = −0.93, R^2 = 0.89).

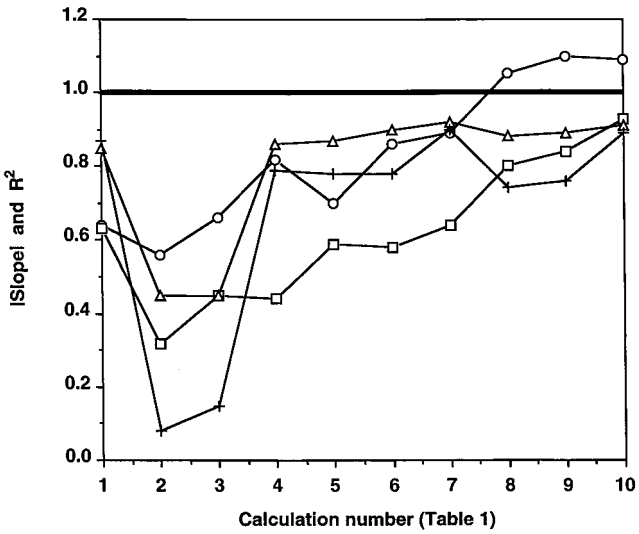

Figure 10. Graph showing the changes in |slope| and R^2 for the correlations between theory and experiment for C^{α} and C^{β} sites in valine residues in calmodulin, SNase, and ubiquitin: ○, C^{α} slope; □, C^{β} slope; △, C^{α} R^2; and +, C^{β} R^2. The *x*-axis refers to the calculations (**1**−**10**) reported in Table 1.

accessible via relaxation,[31] and for peptide model systems, a number of helix and sheet-like tensors have recently been deduced and predicted theoretically.[29,30]

We show in Tables S2 and S3 C^{α} and C^{β} shielding tensor elements for 12 representative valine residues computed with CHF (Texas) and DFT (deMon) methods, and these individual

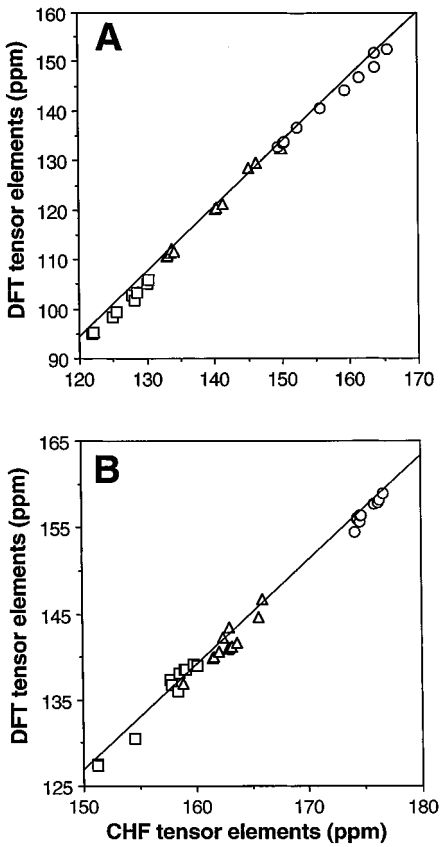

Figure 11. Graphs showing comparisons between $^{13}C^{\alpha}$ and $^{13}C^{\beta}$ valine shielding tensor elements computed by using CHF and DFT methods: (A) C^{α} and (B) C^{β}. The CHF method used the Texas program with a locally dense basis while the DFT calculations used a uniformly dense IGLO-II basis and the PW91 functional: □, σ_{11}; △, σ_{22}; ○, σ_{33}. In graph A, the slope is 1.33 and the R^2 value is 0.997. In graph B, the slope is 1.19 and the R^2 value is 0.992.

tensor elements are plotted against each other, for C^{α} and C^{β}, in graphs A and B in Figure 11. For C^{α}, there is clearly a very major decrease in shielding in the DFT calculations, and a similar effect is also seen for C^{β}, graphs A and B in Figure 11. In addition, the more shielded tensor elements remain at about the same shielding, while the less shielded elements become even less shielded in the DFT calculations. The effect is, however, quite monotonic, as shown by the very high R^2 values: for C^{α} we find a slope of 1.33, R^2 = 0.997; for C^{β}, the slope is 1.19, R^2 = 0.992. Interestingly, it should be noted that with C^{α} in alanine, the slope of the experiment versus CHF theory tensor element correlation is 1.28,[30] close to that (1.33) seen with the valine C^{α} DFT versus CHF result, Figure 11A, implying that CHF, DFT, and experimental results are all related by small overall scaling factors. This is an important result since it means that eventually exact isotropic chemical shifts as well as shift tensor elements (δ_{11}, δ_{22}, δ_{33}) can be obtained from either CHF or DFT methods by using small offset and scaling corrections determined experimentally.[30]

Also of great interest is the observation that the α-helical and β-sheet tensor elements are very different. This is shown in Figure 12 in which we present the G94 DFT tensor elements for the 12 valine residues given in Table S2. Figure 12 indicates that sheet residues typically have a 50% larger chemical shift anisotropy than do helical residues, and that the familiar ∼5 ppm helix-sheet isotropic shift differences seen empirically originate from quite complex changes in the individual tensor elements—at least in the case of valine. The results of some 3000 additional shielding calculations which support this idea will be reported elsewhere in more detail.[29]

(30) Heller, J.; Laws, D. D.; King, D. S.; Wemmer, D. E.; Pines, A.; Havlin R. H.; Oldfield, E. *J. Am. Chem. Soc.* **1997**, *119*, 7827−7831.
(31) Bax, A. Private communication.

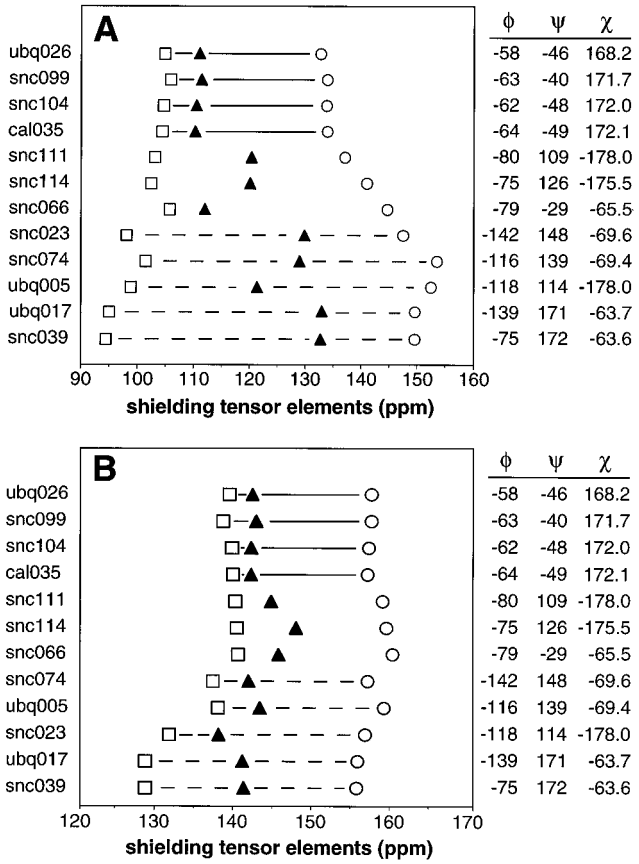

Figure 12. Shielding tensor elements for C^{α} and C^{β} in 12 valine fragments showing changes in (□) σ_{11}, (▲) σ_{22}, and (○) σ_{33} as a function of fragment structure. Shieldings were computed with Gaussian 94 using a locally dense basis and a BPW91 functional and are from Table 5 in the text: (A) C^{α}; and (B), C^{β}. The solid horizontal bars join the regular helices (with $\chi_1 = 180°$) and the dotted lines join the sheet-like structures. The actual ϕ, ψ, χ_1 values are indicated (ϕ, ψ, χ_1).

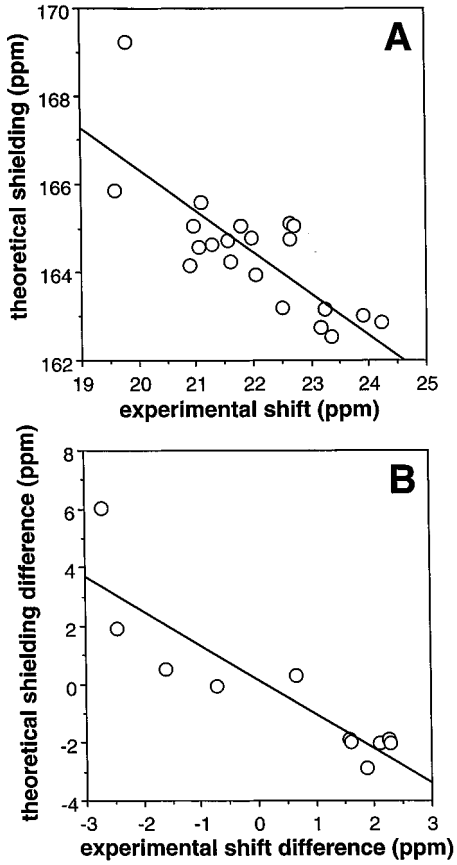

Figure 13. Graph showing experimental C^{γ} shift versus theoretical shielding results for calmodulin and ubiquitin. (A) Experimental versus theoretical C^{γ} results, with stereospecifically assigned $C^{\gamma 1}$, $C^{\gamma 2}$ shifts. G94/DFT calculation with G94 geometry optimized fragments. Slope = 0.94, $R^2 = 0.61$. (B) As in graph A but the experimental $|\delta C^{\gamma_2} - \delta C^{\gamma_1}|$ value is plotted versus the $|\sigma C^{\gamma_2} - \sigma C^{\gamma_1}|$ computed value. Slope = 1.18, $R^2 = 0.79$.

The γ-Carbon Problem

We finally present results on the shifts of the γ-carbons in valine. Here, it seemed likely that it might be rather difficult to accurately evaluate C^{γ} shifts, since many valines have small side-chain (C^{γ}) order parameters,[32] and might be expected to undergo significant motional averaging, making shift calculations intractable. Indeed, in initial studies with standard X-ray structures, we found little correlation between experimental C^{γ} shifts and predicted shielding, but moderate correlations were obtained when the energy selected conformations discussed above were used. We evaluated the carbon-13 shieldings for both C^{γ_1} and C^{γ_2}, which for calmodulin and ubiquitin have been specifically assigned.[32−34] Figure 13A and Table S4 show the calculated shieldings in Gaussian 94 with the BPW91 functional and the 6-311++G(2d,2p) basis set on all atoms, versus the experimental shifts, for all C^{γ_1} and C^{γ_2} in calmodulin and ubiquitin. The slope is good (0.94) as is the intercept (185.10 ppm), but the R^2 value is quite poor, $R^2 = 0.61$. This is not particularly surprising, since the shift range for C^{γ} is small, only 4−5 ppm, compared with a ∼7 ppm range for C^{β} and a ∼10 ppm range for C^{α}. Plus, the order parameters decrease from C^{α} to C^{β} to C^{γ} (more motion), there may be stronger inter-residue interactions for the γ carbons, such as ring-current effects, and finally, any shift referencing effects will be more significant for the smaller shift range. The latter effect can be eliminated by looking at the shift differences $|(\delta C^{\gamma_2} - \delta C^{\gamma_1})|$ and the shielding differences $|\sigma C^{\gamma_2} - \sigma C^{\gamma_1}|$, Figure 13B. Here, the slope is 1.18, slightly worse than the 0.91 of Figure 13A, but the R^2 value improves to $R^2 = 0.79$. We have also calculated the C^{γ} isotropic shieldings with deMon with the PW91 exchange-correlation functional and the IGLO-II orbital basis sets on all atoms, and with point charges. The slope of 0.98 is a slight improvement over the Gaussian 94 DFT calculation, but the R^2 of 0.52 is worse. The slope of the shielding differences versus shift differences graph is 1.20, and the R^2 is 0.79. Interestingly, the large shielding differences predicted for Val 17 in ubiquitin (∼−6 ppm, Figure 13B) ($\chi_1 = -62.5°$, sheet 1) are not seen experimentally, suggesting the influence of motional effects, in this case.

To explore the origins of the C^{γ} shifts in more depth, we next evaluated the effects of the χ_1 torsion on C^{γ} shieldings, Figure 14. Here, we show the computed DFT/G94 shieldings for C^{γ_1} and C^{γ_2} as a function of χ_1 for three typical structures: helical ($\phi = -62°$, $\psi = -41°$), sheet 1 ($\phi = -136°$, $\psi = 143°$), and sheet 2 ($\phi = -75°$, $\psi = 126°$). Similar results were obtained with the CHF approach (Texas program), with the slopes of the DFT versus CHF results ranging from 1.03 to 1.19 (data not shown). Interestingly, the results of Figure 14 indicate that C^{γ_1} is more shielded than C^{γ_2} in all three structures, for $\chi_1 = 180°$, while it is substantially deshielded in all three structures for $\chi_1 = -60°$, with the largest effect being seen in the sheet 1 region. The results of Figure 14 suggest that it may also be possible to refine χ_1 even further by simultaneously optimizing χ_1 with respect to C^{α}, C^{β}, and ΔC^{γ}. However, this was not

(32) Wand, A. J.; Urbauer, J. L.; McEvoy, R. P. *Biochemistry* **1996**, *35*, 6116−6125.
(33) Vuister, G. W.; Wang, A. C.; Bax, A. *J. Am. Chem. Soc.* **1993**, *115*, 5334−5335.
(34) Yamazaki, T. Private communication.

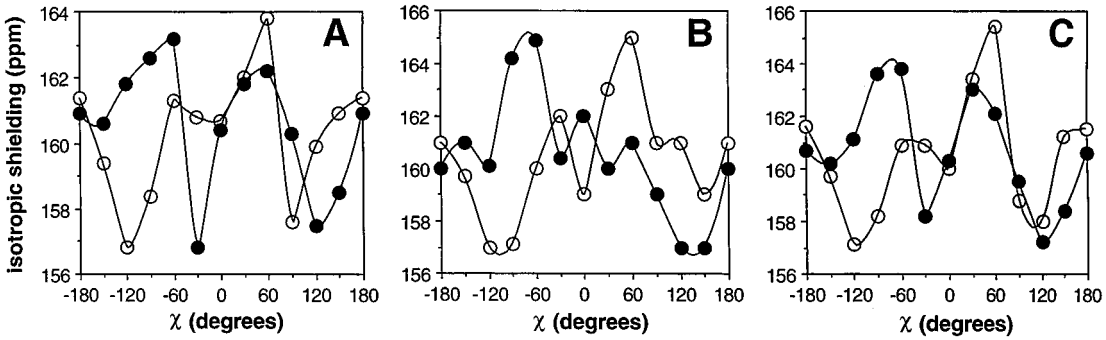

Figure 14. Graph showing χ_1 conformational dependence of C^{γ_1} and C^{γ_2} shifts in *N*-formylvaline amide for (A) helical ($\phi = -62°$, $\psi = -41°$) and, (B) sheet 1 ($\phi = -136°$, $\psi = 143°$) and (C) sheet 2 ($\phi = -75°$, $\psi = 126°$) fragments. DFT calculations were done with Gaussian 94, using the uniformly dense basis set (6-311++G(2d,2p)), as described in the text: (○), C^{γ_1} and (●) C^{γ_2}.

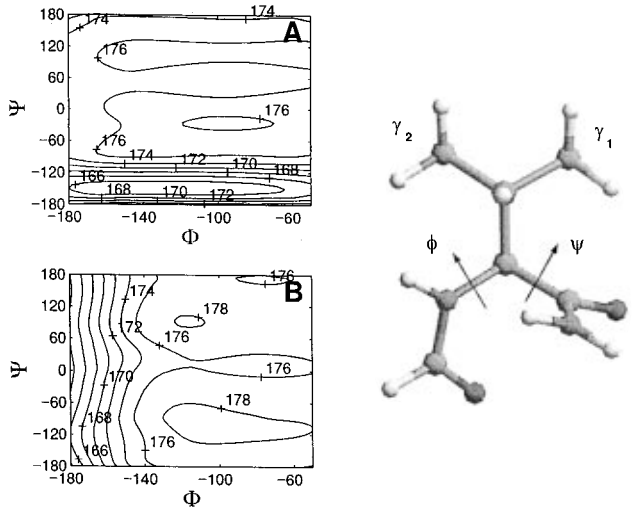

Figure 15. $^{13}C^{\gamma}\phi,\psi$ shielding surfaces for (A), C^{γ_1} and (B) C^{γ_2} atoms in *N*-formylvaline amide, calculated with CHF (Texas program) with a locally dense basis set, shown together with a representative valine fragment.

attempted, given the small number of data points available for proteins having both high-resolution X-ray (ϕ,ψ) structures and stereospecifically assigned C^{γ}, together with the high probability that dynamical and interresidue effects will often influence C^{γ} shielding. Use of energy selected conformers does, however, provide the first relatively good prediction of valine C^{γ} shifts and shift differences in proteins, which has not been possible previously.

Finally, we have investigated the effects of ϕ,ψ on C^{γ_1} and C^{γ_2} shielding, at the three χ_1 minima for valine. Results for the isotropic shielding for C^{γ_1} and C^{γ_2} for $\chi_1 = 180°$ are shown in Figure 15, together with a schematic of the valine fragment used in the calculations. As may be seen from Figure 15, the shielding of C^{γ_1} is very sensitive to the ψ torsion, while that of C^{γ_2} is sensitive to the ϕ torsion. Examination of the molecular structure of the valine residue clearly indicates rotation of the ψ angle brings the associated peptide plane relatively close to C^{γ_1}, while rotation about ϕ brings the other peptide plane close to C^{γ_2}. Thus, the responses of C^{γ_1} and C^{γ_2} to ϕ,ψ can be readily appreciated.

Conclusions

The results we have presented above are of interest since they represent the first in-depth quantum chemical study of C^{α}, C^{β}, and C^{γ} chemical shifts in a series of proteins. Our results show that empirical shielding surfaces do not enable highly accurate shift predictions, neither do standard X-ray structures, because of "noise" associated with the presence of high-energy conformers and possible crystal−solution structural differences. However, our results also indicate that correct global (-60°,180°) conformers can be selected based on purely energetic considerations, and that further albeit small improvements in χ_1 and bond lengths can be deduced via geometry optimization. These refined structures have permitted the accurate and precise prediction of C^{α} and C^{β} chemical shifts in 19 valine residues in three proteins, with more modest correlations for C^{γ}. Charge field effects are small, and give only a minor improvement. The R^2 values obtained by using Hartree−Fock and density functional theory are very similar, but the slopes of the theoretical versus experimental correlations are further improved by using DFT with large, uniform basis sets. These shift improvements are shown to originate in uniform changes in all C^{α}, C^{β} tensor elements, rather than a particular element, the effects increasing with increasing paramagnetic shift.

As discussed in the Introduction, we have tested the hypothesis that backbone structures of proteins in solution are generally well described by ϕ,ψ values taken from high-resolution X-ray crystallographic structures, but that χ_1 torsions (in valine) are less well described. Our results support this hypothesis, as demonstrated by our ability to now calculate C^{α}, C^{β}, and ΔC^{γ} shifts with energy-selected structures, with excellent overall accord between theory and experiment. This approach should find utility in both structure refinement and prediction, in both solution and the solid-state.[29,31]

Acknowledgment. We are grateful to Professors P. Pulay and J. F. Hinton and Dr. K. Wolinski for providing their Texas programs and Professor D. R. Salahub and Drs. V. Malkin, O. Malkina, and E. Proynov for providing their deMon program. We thank Professor A. C. de Dios for calculating the results shown in Figure 15. J.G.P. was supported by an American Cancer Society Postdoctoral Fellowship (Grant No. PF-4141).

Supporting Information Available: Listings of calculated energies of *N*-formylvaline amide fragments in calmodulin, Staphylococcal nuclease, and ubiquitin at X-ray and at standard geometries (Table S1), computed shielding tensor elements for C^{α} (Table S2) and C^{β} (Table S3), and experimental and computed C^{γ_1}, C^{γ_2} isotropic shifts for calmodulin and ubiquitin (Table S4) (5 pages). See any current masthead page for ordering and Internet access instructions.

JA971461W